Stator winding fault detection of permanent magnet synchronous motors based on the bispectrum analysis

Przemysław PIETRZAK⬤ and **Marcin WOLKIEWICZ**⬤*

Wrocław University of Science and Technology, Department of Electrical Machines, Drives and Measurements, Wybrzeże Wyspiańskiego 27, 50-370 Wrocław, Poland

Abstract. The popularity of high-efficiency permanent magnet synchronous motors in drive systems has continued to grow in recent years. Therefore, also the detection of their faults is becoming a very important issue. The most common fault of this type of motor is the stator winding fault. Due to the destructive character of this failure, it is necessary to use fault diagnostic methods that facilitate damage detection in its early stages. This paper presents the effectiveness of spectral and bispectrum analysis application for the detection of stator winding faults in permanent magnet synchronous motors. The analyzed diagnostic signals are stator phase current, stator phase current envelope, and stator phase current space vector module. The proposed solution is experimentally verified during various motor operating conditions. The object of the experimental verification was a 2.5 kW permanent magnet synchronous motor, the construction of which was specially prepared to facilitate inter-turn short circuits modelling. The application of bispectrum analysis discussed so far in the literature has been limited to vibration signals and detecting mechanical damages. There are no papers in the field of motor diagnostic dealing with the bispectrum analysis for stator winding fault detection, especially based on stator phase current signal.

Key words: fault diagnosis; condition monitoring; inter-turn short circuits; permanent magnet synchronous motor; bispectrum; fast Fourier transform.

1. INTRODUCTION

Permanent magnet synchronous motors (PMSMs) are attracting more and more attention in modern drive systems. This growing popularity is related to the fact that they are characterized by high power density, high reliability, high efficiency, low noise, and a wide speed range [1]. PMSMs have been widely used in various applications such as automotive, aerospace, home appliances, robotics, and transportation [2, 3].

Despite their high reliability, PMSMs like other types of electric motor types used in drive systems, are prone to various types of faults during normal operation [4]. The experience of repair centers, manufacturers, and academic studies shows that the approximated faults distribution of electric motors is as follows [5–7]:

- 45% – bearing faults,
- 35% – stator faults,
- 10% – rotor faults,
- 10% – others.

Although bearing faults are the most common cause of motor failures, stator winding faults are much more dangerous due to their destructive character. Damage to the stator winding most

commonly starts with an inter-turn short circuit between adjacent turns. This imperceptible short circuit may spread over the whole winding in a very short time and cause critical motor damage and emergency stop of the drive system [8].

Due to the nature of the PMSM stator winding fault, it must be detected effectively and at a very early stage to avoid costly repairs and downtimes. Nevertheless, in order to be able to conduct effective detection of motor failures, it is necessary to use appropriate diagnostic methods. Most of them are based on the processed diagnostic signal [9]. Diagnostic signals are those that contain information about the technical condition of the motor, such as phase current, voltage, mechanical vibration, acoustic signal, and temperature [10].

The processing of the diagnostic signal facilitates the extraction of fault features and is performed with the use of various methods that can carry out the analysis in the time, frequency, or time-frequency domain [11]. In the case of stator winding faults, the most popular method is stator phase current frequency-domain spectral analysis using the fast Fourier transform (FFT) [12–15]. It is one of the classic diagnostic methods known for many years. Nevertheless, due to the increasing computing power of microcontroller-based embedded systems, even low-budget ones, in recent years the use of more advanced mathematical apparatuses has been gaining popularity. This group includes transforms carrying out analysis in the time-frequency domain. In the past, advanced methods were successfully applied to the extraction of the PMSM stator

*e-mail: marcin.wolkiewicz@pwr.edu.pl

Bull. Pol. Acad. Sci. Tech. Sci., vol. 70, no. 2, p. e140556, 2022

1

winding faults symptoms, such as short time Fourier transform (STFT) [16], continuous wavelet transform (CWT) [17], discrete wavelet transform (DWT) [14, 18], Hilbert Huang transform (HHT) [19] and Wigner-Ville distribution (WVD) [20]. A novel inter-turn faults detection method that utilizes time-frequency analysis based on the Gabor order tracking is proposed in [21].

The use of high-order transforms (HOTs) such as multiple signal classification (MUSIC) [22–24] and bispectrum [25–28] for the detection of electric motor faults is also widely described in the literature. Nevertheless, there is a lack of papers dealing with the topic of PMSM stator winding fault detection using stator phase current bispectrum analysis. This is a topic that has been largely under-researched so far. Therefore, these issues are becoming more and more attractive also due to the dynamically developing methods of automatic inferring about the condition of the motor, especially based on classic machine learning algorithms, shallow and deep neural networks (DNNs).

In the last years, papers have been published that present the combination of advanced signal processing methods with DNNs, such as CNN, for motor fault diagnosis. They are mainly based on signal processing algorithms, the result of which can be presented as an image [29–31]. The use of bispectrum analysis may also allow us to collect data sets containing extracted symptoms that can be successfully used to train the artificial intelligence-based fault detectors and classifiers. Moreover, it should be highlighted that fault symptoms extraction, feature processing, and data collection are crucial parts of motor condition monitoring [32].

The contribution of this work is the application of the bispectrum analysis of stator phase current, stator phase current envelope, and state phase current space vector module in symptoms extraction of inter-turn short circuits in PMSM stator winding. The use of this advanced HOT has been compared with the classical method – FFT. Both signal processing methods were tested for a PMSM drive system under variable load torque and rotation speed. The use of bispectrum analysis of diagnostic signals based on the stator phase current under various operating conditions has not been investigated in the literature so far and may be very helpful in the development of diagnostic systems that require a database of extracted symptoms to train the models on which they are based.

2. BISPECTRUM ANALYSIS

The high order spectral analysis (HOSA) which is based on HOTs has been known for many years and is used mainly in signal processing [33]. Nevertheless, due to the rapidly increasing computing power of microcontrollers, their availability in the market, and decreasing prices, the application of HOSA methods in the field of fault diagnostics is an interesting issue.

Bispectrum is one of the most promising HOTs, the first application of which is dated to 1962 (analysis of nonlinear interaction of ocean waves) [34]. Since then, it has found application in many areas such as economics, fluid mechanics, plasma physics, oceanography, and biomedicine [35].

While the FFT decomposes the signal by its frequency, the bispectrum analysis allows one to get information regarding specific interactions between the different frequency components. Moreover, it provides an analysis of square and cubic nonlinearities. Studying the non-linear interaction between signal harmonics can be a useful way to amplify their respective effects and make the extraction of the corresponding fault symptoms easier [36].

Another advantage of this transform is that, after the signal processing, the information about the phase of the signal components is not lost. It facilitates the detection of phase relationships between its components.

HOTs are described by moments and cumulants of order $n > 2$. To obtain the bispectrum of the signal it is necessary to perform the FFT on the cumulant or moment of $n = 3$. Due to the properties described in the further part of this paper, the most popular method is the cumulant-based approach.

For a stationary random discrete signal, the third-order cumulant is a two-variable function τ_1, τ_2. The relation between the cumulant and random signal $x(n)$ is defined as follows [28]:

$$c_3^x(\tau_1, \tau_2) = \mathrm{E}[x(n), x(n+\tau_1), x(n+\tau_2)], \qquad (1)$$

where τ_1, τ_2 – time intervals, $n = 0, \pm 1, \pm 2$ – sample number, E[ ] – expected or mean value.

Next, the signal bispectrum is determined by the double Fourier transform of the third-order cumulant [37]:

$$B_x(f_1, f_2) = \sum_{\tau_1=-\infty}^{\infty} \sum_{\tau_2=-\infty}^{\infty} c_3^x(\tau_1, \tau_2) \mathrm{e}^{-2\pi f_1 \tau_1} \mathrm{e}^{-2\pi f_2 \tau_2}, \qquad (2)$$

which can be expressed as [37]:

$$B_x(f_1, f_2) = \mathrm{E}[X(f_1), X(f_2), X^*(f_1 + f_2)], \qquad (3)$$

where $X(f)$ is the Fourier transform of the $x(n)$ and $X^*(f)$ is its conjugate.

Bispectrum, which is based on the third-order cumulant, retains its properties. The most important is the argument symmetry, which means that a change in the argument order does not change bispectrum value [37, 38]:

$$\begin{aligned} B_x(f_1, f_2) &= B_x(f_2, f_1) = B_x(-f_2, -f_1) \\ &= B_x(f_1, -f_1 - f_2) = B_x(-f_1 - f_2, f_2) \\ &= B_x(-f_1 - f_2, f_1) = B_x(f_2, -f_1 - f_2). \end{aligned} \qquad (4)$$

The symmetric regions of the bispectrum are shown in Fig. 1. Considering the properties described by equation (4), the analysis of frequency component amplitudes during the experimental verification was limited to one non-redundant triangular region (I) – the principal domain. This area is marked in green in Fig. 1. It can be described as follows:

$$\xi = \{(f_1, f_2) \colon 0 \leq f_2 \leq f_1 \leq \frac{f_e}{2}; \ f_1 + f_2 \leq \frac{f_e}{2}, \qquad (5)$$

where f_e is the sampling frequency.

2

Bull. Pol. Acad. Sci. Tech. Sci., vol. 70, no. 2, p. e140556, 2022

Stator winding fault detection of permanent magnet synchronous motors based on the bispectrum analysis
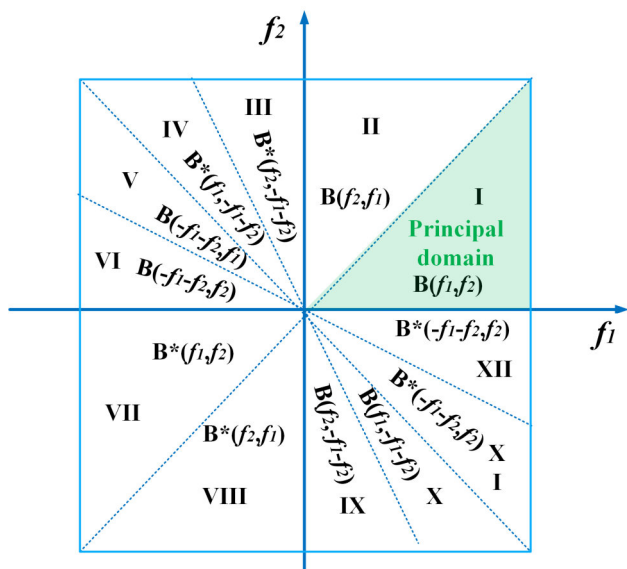

Fig. 1. Bispectrum symmetry regions

3. EXPERIMENTAL SETUP

The object of the experimental tests was a 2.5 kW PMSM powered by a voltage source inverter (VSI) and operating in a closed-loop motor control structure. To generate the load torque a second PMSM with nominal power of 4.7 kW was used. The test stand is shown in Fig. 2. The motor shown on the right side is the loading motor, while the second one is the tested PMSM whose parameters are listed in Appendix A. The construction of the tested PMSM was specially prepared to enable inter-turn short circuits modelling of a selected number of turns in phase B of the stator winding. The diagram of the derived phase terminals is shown in Fig. 3. Each of the stator winding phases consists of two coils – 125 turns each. Direct inter-turn short circuits were done by connecting the selected tabs on the terminal board with a wire. During the measurements, a maximum of three turns were short circuited. It accounts for 1.6% of all turns in the phase. The stator phase currents were measured with current transducers – LEM LA 25-NP, the output signals of which were passed to the DAQ NI PXI-4492 data acquisition system by National Instruments (NI, Austin, TX, USA). The DAQ card was placed on the industrial PC – NI PXI 1082.
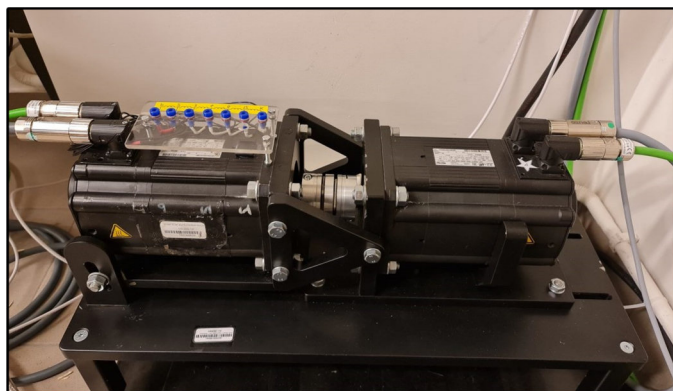

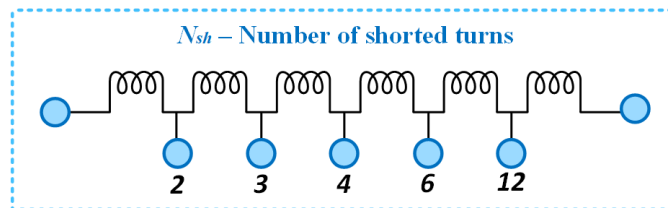**Fig. 2.** Experimental stand

Fig. 3. Diagram of the stator winding phase terminals

Pre-processing of diagnostic signals was carried out in the LabVIEW programming environment. Lenze Engineer Software was used to control the tested PMSM, whereas VeriStand was used to set the load torque. The block diagram of the experimental setup is shown in Fig. 4.
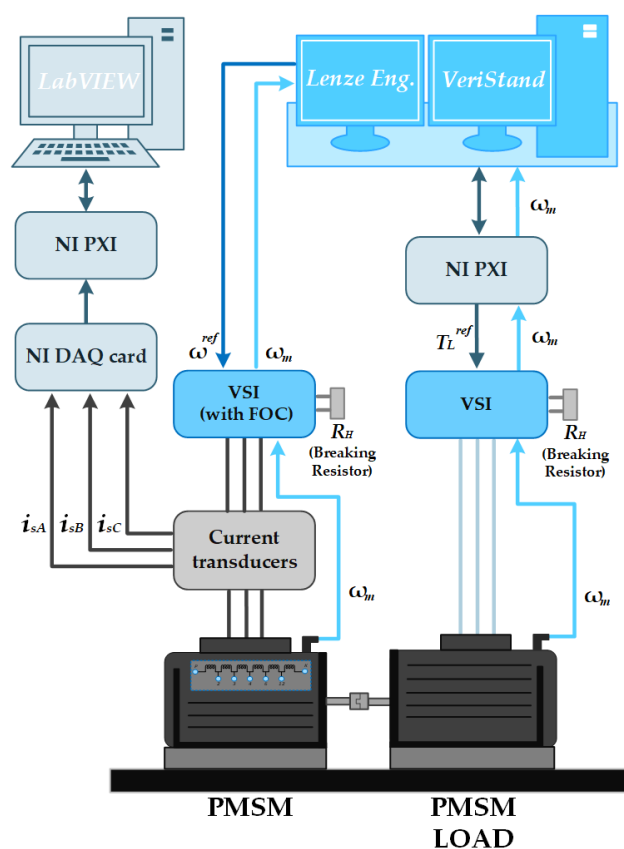

Fig. 4. Block diagram of the experimental setup

4. EXPERIMENTAL TEST SCENARIOS AND RESULTS

The experimental verification of the bispectrum analysis application for PMSM stator winding detection was preceded by an FFT analysis of the proposed diagnostic signals. The analyzed diagnostic signals are stator phase current, stator phase current envelope, and the vector module of stator phase current space. The diagnostic application responsible for the data acquisition and signal pre-processing (bispectrum analysis of the selected diagnosis signals) is developed in the LabVIEW programming environment with the use of the *Advanced Signal Processing Toolkit*.

P. Pietrzak and M. Wolkiewicz

Determination of the stator phase current envelope may allow us to extract current fluctuations caused by the stator faults. The stator phase current envelope was calculated as follows:

$$i_s^H(t) = \sqrt{i_s^2(t) + H^2[i_s(t)]}, \qquad (6)$$

where $H[i_s(t)]$ – Hilbert transform of phase current signal:

$$H[i_s(t)] = \frac{1}{\pi} \int_{-\infty}^{+\infty} \frac{i_s(t)}{i - \tau} \, d\tau. \qquad (7)$$

The spectral analysis of the stator phase current space vector module has been used in the past to detect induction motor stator faults and is known in the literature under the EPVA abbreviation (Extended Park's Vector Approach) [39]. The space current space vector module is defined in accordance with the following equation:

$$|i_s| = \sqrt{i_{s\alpha}^2 + i_{s\beta}^2}, \qquad (8)$$

where $i_{s\alpha}$, $i_{s\beta}$ are the stator phase current components in α-β reference frame. It should be highlighted that the bispectrum analysis of $|i_s|$ has not been discussed in the literature so far.

Experimental tests were carried out for various values of the load torque $(0 \div 1)$ T_N and the power supply frequencies $(50 \div 100)$ Hz. It facilitated examining the influence of motor operating conditions on the extracted inter-turn short circuits symptoms.

4.1. FFT analysis

The FFT-based spectral analysis of the diagnostic signal is one of the most popular techniques used in electric motor faults diagnosis. In the FFT spectra, the changes of harmonic amplitudes characteristic for the stator winding fault are searched. Tracking the value of these amplitudes may allow for motor condition monitoring.

4.1.1. Stator phase current

In the first step, the FFT analysis of the stator phase current signal was carried out. Figure 5 shows the spectra of the stator phase current (phase B) for the motor operating at nomi-
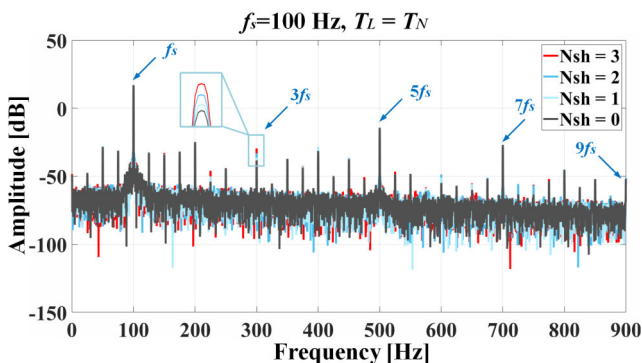
nal power supply frequency $f_s = f_{sN}$ and nominal load torque $T_L = T_N$, for an undamaged stator winding and with 1, 2, and 3 shorted turns – N_{sh}. In these spectra, a significant increase in the amplitude of the third harmonic can be observed after the stator winding fault.

The greater the increase, the greater the number of shorted turns. This is the only component the amplitude of which increases consequently with the increasing N_{sh}.

In order to assess the exact impact of the damage on the amplitude of a given frequency component and the subsequent comparison of the increases between other diagnostic signals and the bispectrum analysis, the increase in the amplitude for a given N_{sh} in relation to the value for an undamaged winding is analyzed:

$$A_{\text{DIFF}}(f_c) = A_{\text{Damaged}}(f_c) - A_{\text{Undamaged}}(f_c), \qquad (9)$$

where f_c is the characteristic failure frequency component, A_{Damaged}, $A_{\text{Undamaged}}$ are the amplitudes of f_c component for damaged and undamaged motor respectively.

The effect of N_{sh} and T_L on the amplitude value of the $3f_s$ frequency component is shown in Fig. 6, while the dependence on the f_s value is illustrated in Fig. 7. Based on the presented
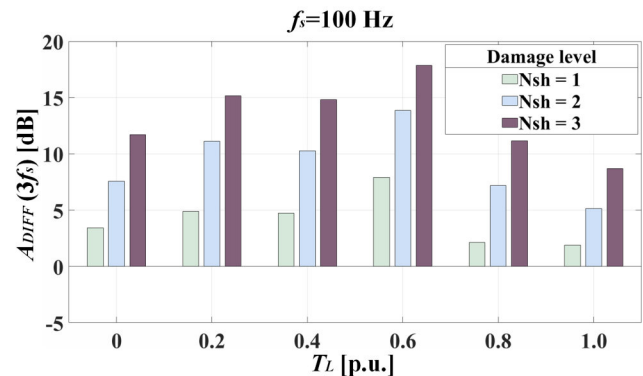

Fig. 6. The impact of N_{sh} in the PMSM stator winding and T_L value ($f_s = 100$ Hz) on the amplitude increase of $3f_s$ frequency component in the stator current spectrum
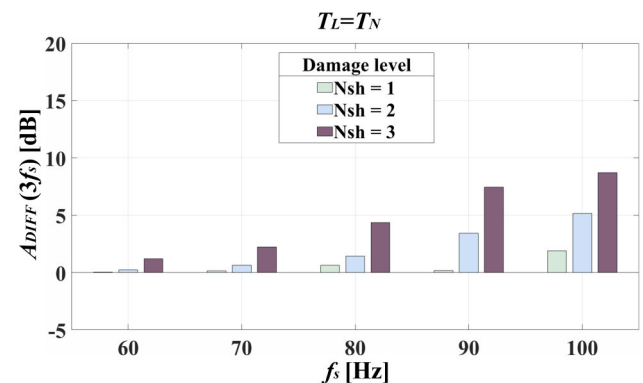

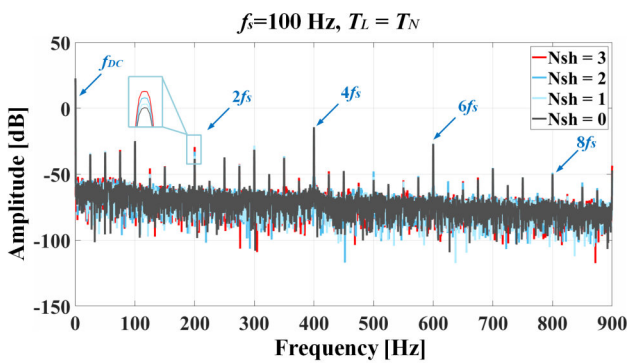**Fig. 5.** The impact of shorted turns in the PMSM stator winding on the stator phase current FFT spectrum ($f_s = 100$ Hz, $T_L = T_N$)

Fig. 7. The impact of N_{sh} in the PMSM stator winding and f_s value ($T_L = T_N$) on the amplitude increase of $3f_s$ frequency component in the stator current spectrum

results it can be concluded that the amplitude increase of the $3f_s$ caused by the stator winding fault is significant (up to 18 dB), especially in the case of motor operating at rotation speed close to the rated value.

However, as the value of the power supply frequency f_s decreases (lower rotation speed than the rated value), the fault sensitivity of this component to damage decreases.

4.1.2. Stator phase current envelope

In the next step, the application of the FFT analysis of the stator phase current envelope signal to the inter-turn short circuits detection was verified. The FFT spectra of the stator phase current envelope for the motor operating with $f_s = f_{sN}$ and $T_L = T_N$, for an undamaged stator winding, and a different number of shorted turns N_{sh} are presented in Fig. 8.

Fig. 8. The impact of shorted turns in the PMSM stator winding on the stator phase current envelope FFT spectrum ($f_s = 100$ Hz, $T_L = T_N$)

In this case, an increase in the amplitude of the second harmonic is visible after the stator winding fault. The effect of N_{sh} and T_L on the $2f_s$ amplitude increase after the inter-turn short circuit is shown in Fig. 9, while the dependence on the f_s is shown in Fig. 10. Based on the bar charts presented in these figures it can be concluded that the amplitude increase of the $2f_s$ caused by the stator winding fault is large (up to 17 dB). However, as in the case of stator phase current spectral analysis, when the value of the power supply frequency f_s decreases
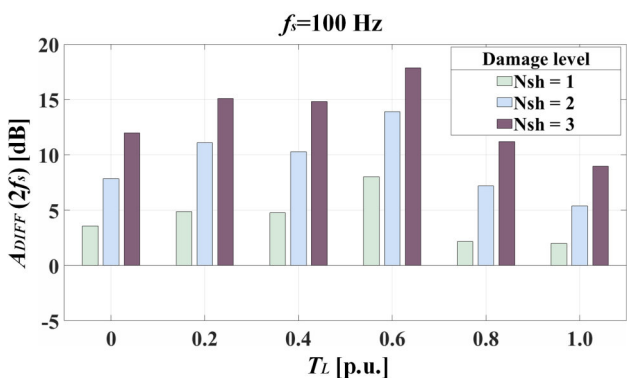

Fig. 9. The impact of N_{sh} in the PMSM stator winding and T_L value ($f_s = 100$ Hz) on the amplitude increase of $2f_s$ frequency component in the stator current envelope spectrum

(lower rotation speed than the rated value), the fault sensitivity of this component to damage decreases.
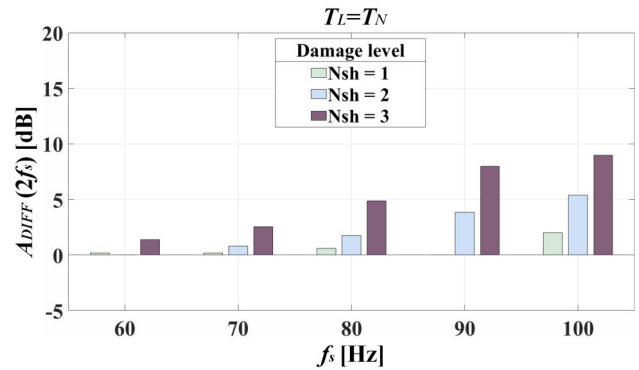

Fig. 10. The impact of N_{sh} in the PMSM stator winding and f_s value ($T_L = T_N$) on the amplitude increase of $2f_s$ frequency component in the stator current envelope spectrum

4.1.3. Stator phase current space vector module

In the last step of this research part, the FFT analysis of the stator phase current space vector module signal was carried out. Figure 11 shows the spectra of the stator phase current space vector module for the motor operating at nominal operation conditions ($f_s = f_{sN}$ and $T_L = T_N$), for an undamaged stator winding and with a different number of shorted turns in one of the coils in phase B. As in the case of the spectral analysis of the stator phase current envelope, the amplitude increase of the $2f_s$ component is very large.
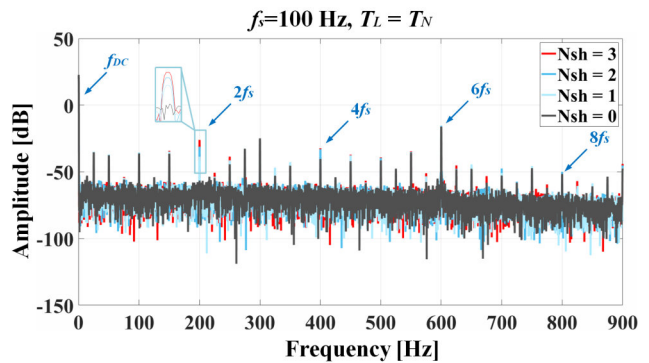

Fig. 11. The impact of N_{sh} in the PMSM stator winding on the stator phase current space vector module FFT spectrum ($f_s = 100$ Hz, $T_L = T_N$)

The influence of N_{sh} and T_L changes on the $2f_s$ amplitude difference compared to the undamaged motor after the inter-turn short circuit is shown in Fig. 12. The effect of the rotation speed (frequency of the supply voltage f_s) is shown in Fig. 13. It can be concluded that the amplitude of the $2f_s$ frequency component is very sensitive to the stator winding faults. The values of increases are much higher compared to the previously described results, especially when the motor is operating at the rated condition – an increase by as much as about 30 dB for 3 shorted turns. Moreover, even at a lower power supply frequency than the rated value, these increases are significant.
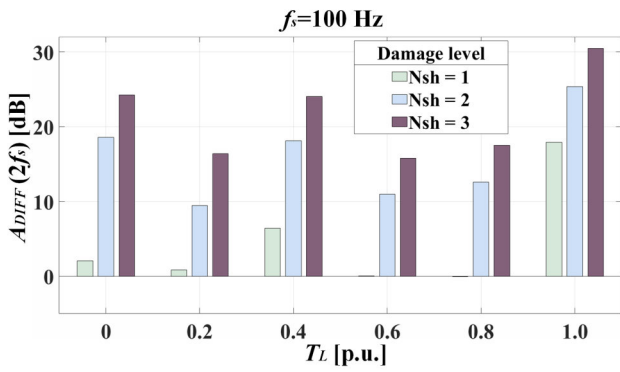
Bull. Pol. Acad. Sci. Tech. Sci., vol. 70, no. 2, p. e140556, 2022

5

Fig. 12. The impact of N_{sh} in the PMSM stator winding and T_L value ($f_s = 100$ Hz) on the amplitude increase of $2f_s$ frequency component in the stator current space vector module spectrum
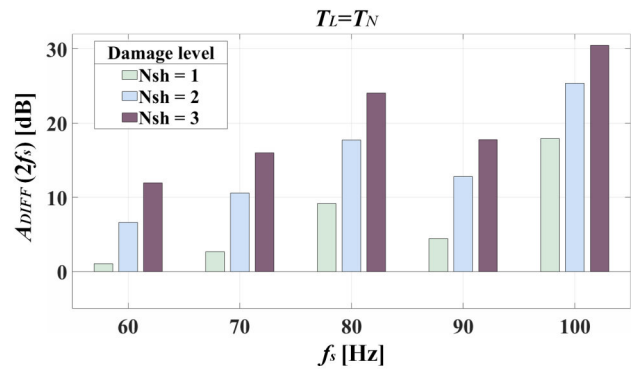

Fig. 13. The impact of N_{sh} in the PMSM stator winding and f_s value ($T_L = T_N$) on the amplitude increase of $2f_s$ frequency component in the stator current space vector module spectrum

4.2. Bispectrum analysis

In the next stage of the research, the bispectrum analysis application of the previously discussed diagnostic signals to the extraction of the inter-turn short circuits was carried out. The use of this HOT is associated with the search for the relationships between the frequencies characteristic to a given fault, which can be distinguished as increases in the amplitudes of the points corresponding to a given frequency pair on the bispectra.

4.2.1. Stator phase current

As with the application of the FFT, the first diagnostic signal analyzed is the stator phase current. 2D and 3D bispectra of the stator current signal for an undamaged PMSM and with 3 shorted turns are presented in Fig. 14 ($f_s = f_{sN}$, $T_L = T_N$). The figure shows a considerable increase in the amplitude value of the points corresponding to the frequency pairs: $(3f_s, 0)$, $(3f_s, f_s)$, and $(3f_s, 3f_s)$. This increase is visible as character-
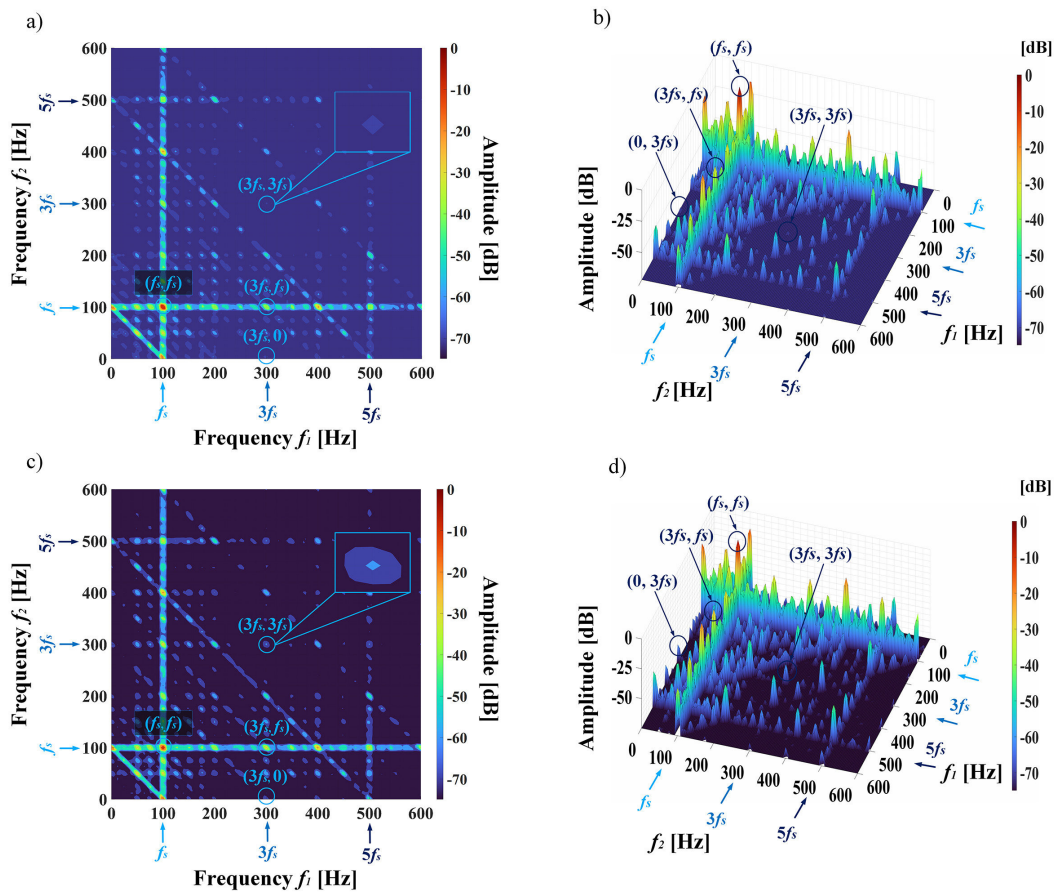

Fig. 14. Three- and two dimensional bispectra of the stator phase current signal for a), b) undamaged stator winding and c), d) 3 shorted turns ($f_s = 100$ Hz, $T_L = T_N$)

6

Bull. Pol. Acad. Sci. Tech. Sci., vol. 70, no. 2, p. e140556, 2022

istic peaks of amplitudes appearing at these points. Based on a thorough analysis of changes in the amplitudes of these points caused by the inter-turn short circuits, it is found that the amplitude of the point $(3f_s, 3f_s)$ is the least sensitive to changes in operating conditions fault indicator.

The effect of N_{sh} and T_L on the amplitude increase of the $(3f_s, 3f_s)$ point on the bispectrum is shown in Fig. 15a, while the dependence on the f_s value is illustrated in Fig. 15b. It can be deduced that the amplitude increase of the $(3f_s, 3f_s)$ peak due to the stator winding fault is visible over the full motor

load torque range (up to 15 dB) and is much greater at lower frequencies (60÷90) Hz than in the case of the FFT analysis, which is an undoubted advantage.

4.2.2. Stator phase current envelope

The 2D and 3D bispectra of the stator current signal for an undamaged PMSM and with 3 shorted turns are presented in Fig. 16 ($f_s = f_{sN}$, $T_L = T_N$). In this case, the increase in the amplitude value of the points corresponding to the frequency pairs: $(2f_s, 0)$ and $(4f_s, 0)$ can be observed. The same as in the case
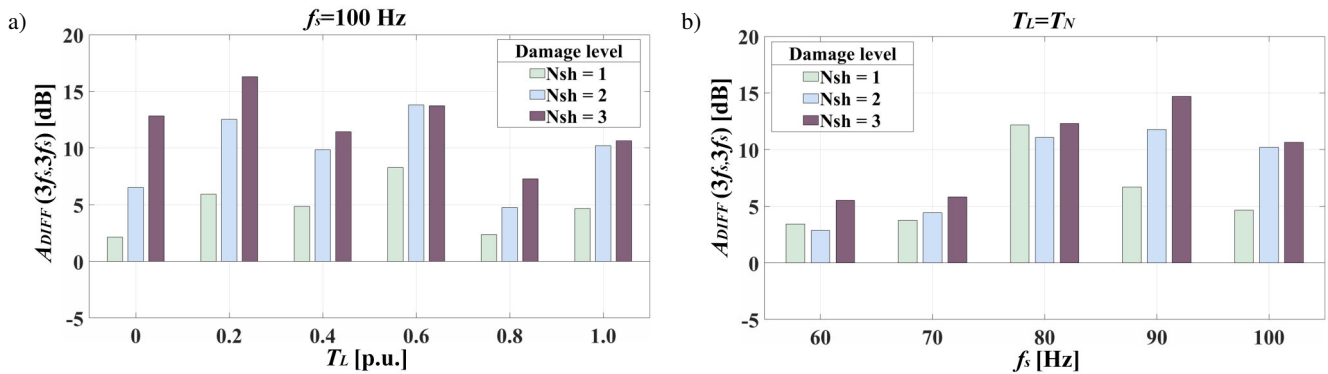

Fig. 15. The impact of N_{sh} in the PMSM stator winding, a) T_L and b) f_s value on the amplitude increase of $(3f_s, 3f_s)$ frequency component in the stator current bispectrum
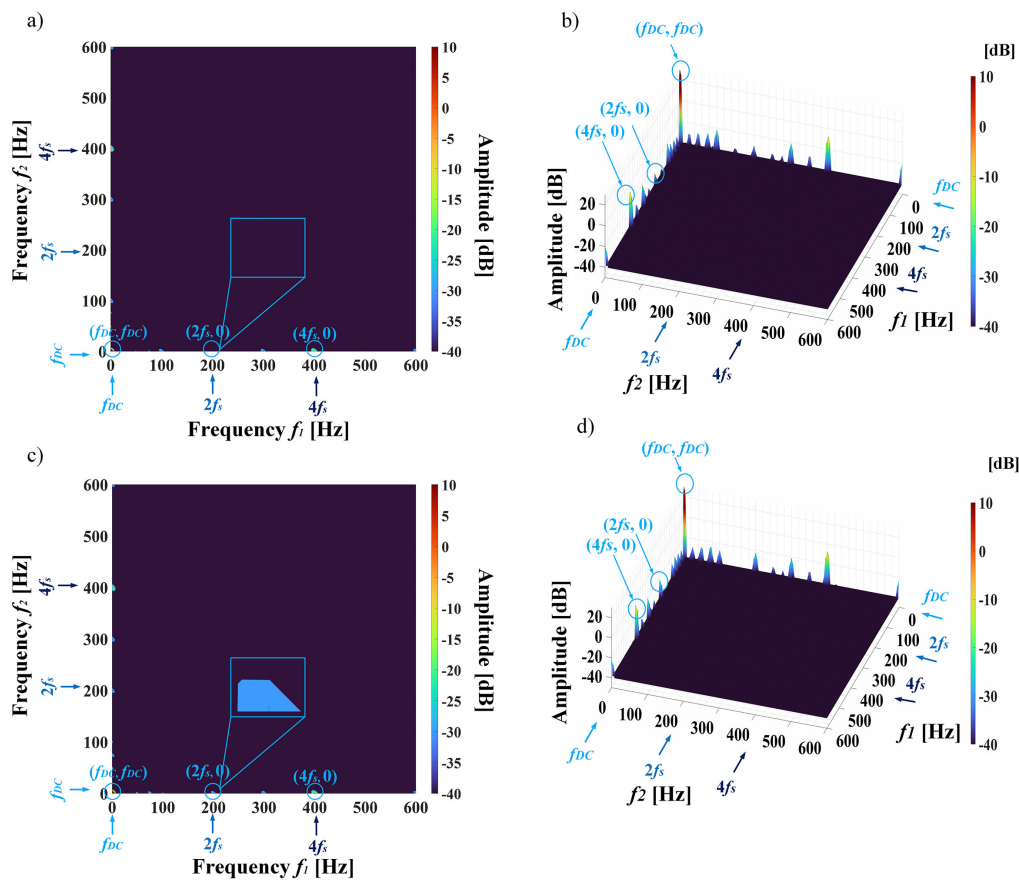

Fig. 16. Three- and two dimensional bispectra of the stator phase current envelope signal for a), b) undamaged stator winding and c), d) 3shorted turns ($f_s = 100$ Hz, $T_L = T_N$)

Bull. Pol. Acad. Sci. Tech. Sci., vol. 70, no. 2, p. e140556, 2022

7

of the stator phase current bispectrum, an analysis of changes in the amplitudes of these peaks caused by the stator winding fault, it is decided that the $(2f_s, 0)$ amplitude is much more sensitive to the failure and least sensitive to the changes in the operating conditions.

The effect of N_{sh} and T_L on the amplitude increase of these points is shown in Fig. 17a, whereas the dependence on the f_s value is presented in Fig. 17b. The results show that the value of $A_{\text{DIFF}}(2f_s, 0)$ caused by the stator winding fault is large for each of the tested load torques and reaches the maximum value

of about 17 dB for 3 shouted turns and as much as 7 dB for one shorted turn. Nevertheless, the susceptibility to damage decreases at f_s lower than 80 Hz.

4.2.3. Stator phase current space vector module

The last diagnostic signal analyzed was the stator phase current space vector module. 2D and 3D bispectra of this signal for an undamaged PMSM and with 3 shorted turns are presented in Fig. 18 ($f_s = f_{sN}, T_L = T_N$). In this case, the increase in the amplitude value of the points corresponding to the frequency
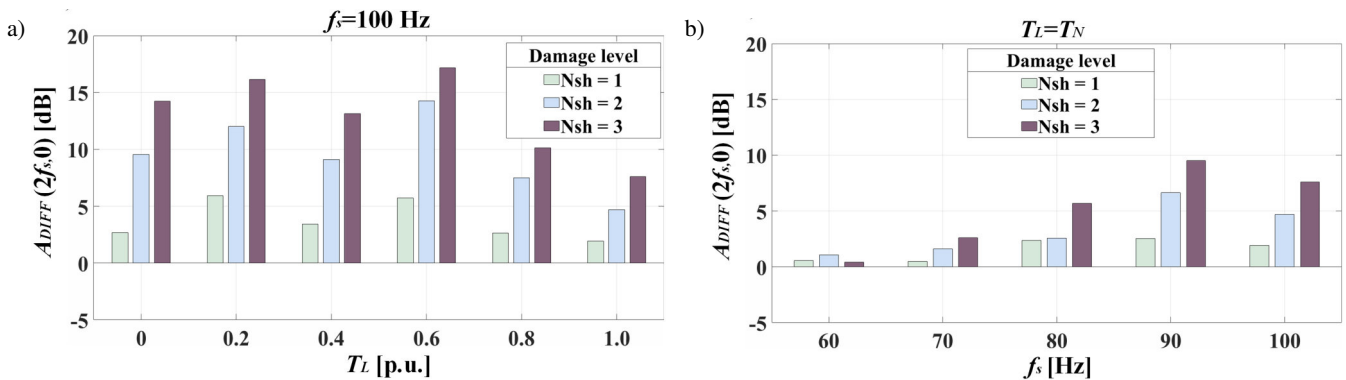

Fig. 17. The impact of N_{sh} in the PMSM stator winding, a) T_L and b) f_s stator current envelope bispectrum value on the amplitude increase of $(2fs, 0)$ frequency component in the stator current envelope bispectrum
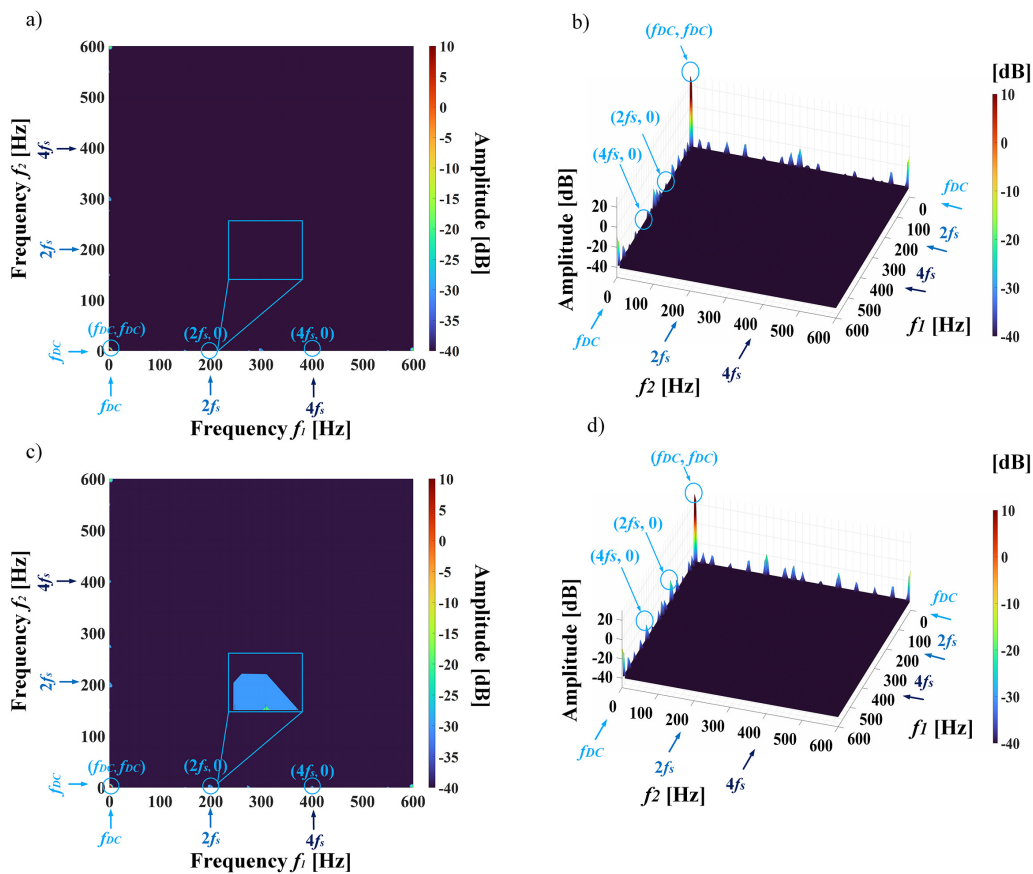

Fig. 18. Three- and two dimensional bispectra of the stator phase current space vector module for a), b) undamaged stator winding and c), d) 3 shorted turns ($f_s = 100$ Hz, $T_L = T_N$)

8

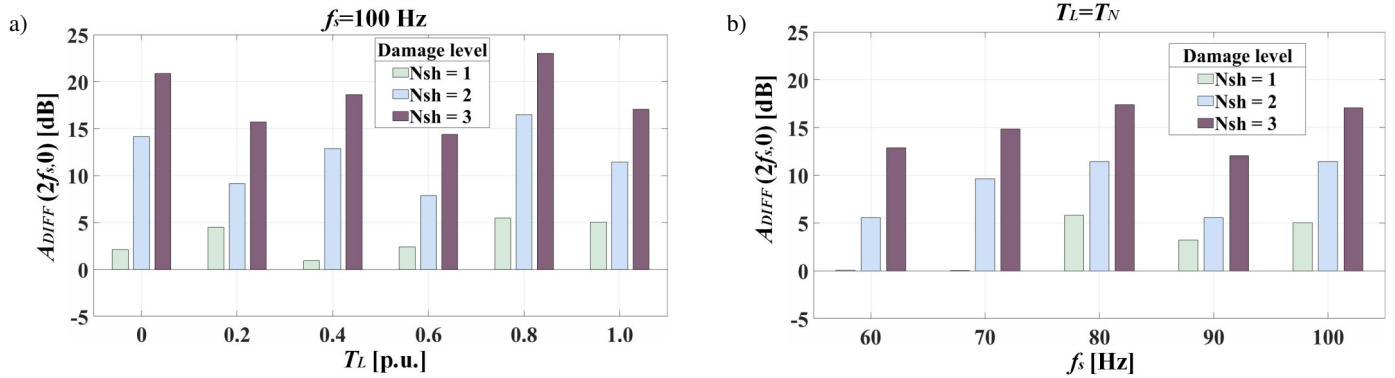Bull. Pol. Acad. Sci. Tech. Sci., vol. 70, no. 2, p. e140556, 2022

Fig. 19. The impact of Nsh in the PMSM stator winding, a) T_L and b) f_s value on the amplitude increase of $(2fs,0)$ frequency component in the stator current space vector module bispectrum

pairs: $(2f_s,0)$ and $(4f_s,0)$ can be observed. Due to the stator winding fault, the increases in both of these points are significant. Nevertheless, taking into account the changing motor operation conditions, the $(2f_s,0)$ component is more promising as the damage indicator.

Figure 19 shows the effect of N_{sh}, T_L and f_s on the amplitude increase of this point. The results show that the value of A_{DIFF}, $(2f_s,0)$, caused by the stator winding fault is higher than in the case of previously analyzed signals. These increases are equal up to 23 dB at the nominal frequency of the supply voltage and as much as 13 dB at a significantly reduced frequency – 60 Hz.

5. CONCLUSIONS

This paper has addressed the issue of PMSM stator winding fault diagnosis. The two signal processing methods: well-known FFT analysis and the bispectrum analysis, which have not been used so far to detect this type of PMSM fault, are proposed to the inter-turn short circuits detection extraction. The analysis has not only been performed for the stator phase current signal but has also been extended to the stator phase current and the stator phase current space vector module, which is a significant contribution to the topic of PMSM electrical failure detection.

The presented experimental research results confirm the effectiveness of the application of the bispectrum analysis of the stator phase current, stator phase current envelope, and stator phase current space vector module to the symptom extraction of the inter-turn short circuits in the PMSM stator winding. Unlike the FFT analysis, which is also useful for the extraction of these symptoms, the bispectrum analysis allows us to extract more than one characteristic failure component for each of the analysed signals. Moreover, it provides higher sensitivity to the failure when the rotation speed (power supply frequency) is significantly lower than the rated value at an early stage, even with one shorted turn in the phase (0.4% of all turns in a phase). Based on the thorough analysis of the results, the most promising is the bispectrum analysis of the stator current space vector module.

The results presented in this paper supplement the missing part of work in the field of motor diagnostics dealing with bis-pectrum analysis for stator winding fault detection, which so far has been limited to applications based on vibration signal and for detecting mechanical damages, mainly of induction motors. Proving that the bispectrum analysis of the stator phase current-based signals allows for the isolation of more symptoms than the FFT can be extremely useful in the development of diagnostic systems based on machine learning models and artificial neural networks, and on the appropriate selection of the input vectors.

APPENDIX

Table 1
Rated parameters of the tested PMSM

Parameter	Symbol	Value
Power	P_N	2500 W
Torque	T_N	16 Nm
Rotation speed	n_N	1500 rpm
Stator phase voltage	U_{sN}	325 V
Stator phase current	I_{sN}	6.6 A
Frequency	f_{sN}	100 Hz
Pole pairs number	p_p	4
Number of turns in one phase	N_s	2×125

REFERENCES

[1] Y. Zuo, X. Zhu, X. Si and C.H.T. Lee, "Fault-Tolerant Control for Multiple Open-Leg Faults in Open-End Winding Permanent Magnet Synchronous Motor System Based on Winding Reconnection," *IEEE Trans. Power Electron.*, vol. 36, no. 5, pp. 6068–6078, May 2021, doi: 10.1109/TPEL.2020.3030237.

[2] X. Zhou, J. Sun, P. Cui, Y. Lu, M. Lu and Y. Yu, "A Fast and Robust Open-Switch Fault Diagnosis Method for Variable-Speed PMSM System," *IEEE Trans. Power Electron.*, vol. 36, no. 3, pp. 2598–2610, March 2021, doi: 10.1109/TPEL.2020.3013628.

[3] Ł.J. Niewiara, T. Tarczewski and L.M. Grzesiak, "Application of extended Kalman filter for estimation of periodic disturbance and velocity ripple reduction," *Bull. Pol. Acad. Sci. Tech. Sci.*, vol. 68, no. 5, pp. 983–995, 2020, doi: 10.24425/bpasts.2020.134649.

[4] M. Krzysztofiak, M. Skowron, and T. Orlowska-Kowalska, "Analysis of the Impact of Stator Inter-Turn Short Circuits on PMSM Drive with Scalar and Vector Control," *Energies*, vol. 14, no. 1, p. 153, Dec. 2020.

[5] A.J. Bazurto, E.C. Quispe and R.C. Mendoza, "Causes and failures classification of industrial electric motor," in *Proc. IEEE ANDESCON*, 2016, pp. 1–4, doi: 10.1109/ANDESCON.2016.7836190.

[6] S. Nandi, H.A. Toliyat and X. Li, "Condition Monitoring and Fault Diagnosis of Electrical Motors – A Review," *IEEE Trans. Energy Convers.*, vol. 20, no. 4, pp. 719–729, Dec. 2005, doi: 10.1109/TEC.2005.847955.

[7] A.H. Bonnett and C. Yung, "Increased Efficiency Versus Increased Reliability," *IEEE Ind. Appl. Mag.*, vol. 14, no. 1, pp. 29–36, Jan.-Feb. 2008, doi: 10.1109/MIA.2007.909802.

[8] P. Pietrzak and M. Wolkiewicz, "On-line Detection and Classification of PMSM Stator Winding Faults Based on Stator Current Symmetrical Components Analysis and the KNN Algorithm," *Electronics*, vol. 10, no. 15, p. 1786, Jul. 2021.

[9] Y. Chen, S. Liang, W. Li, H. Liang, and C. Wang, "Faults and Diagnosis Methods of Permanent Magnet Synchronous Motors: A Review," *Appl. Sci.*, vol. 9, no. 10, p. 2116, May 2019.

[10] M. Skowron, T. Orlowska-Kowalska, M. Wolkiewicz, and C.T. Kowalski, "Convolutional Neural Network-Based Stator Current Data-Driven Incipient Stator Fault Diagnosis of Inverter-Fed Induction Motor," *Energies*, vol. 13, no. 6, p. 1475, Mar. 2020.

[11] L.S. Maraaba, A.S. Milhem, I.A. Nemer, H. Al-Duwaish and M.A. Abido, "Convolutional Neural Network-Based Inter-Turn Fault Diagnosis in LSPMSMs," *IEEE Access*, vol. 8, pp. 81960–81970, 2020, doi: 10.1109/ACCESS.2020.2991137.

[12] K. Kim, "Simple Online Fault Detecting Scheme for Short-Circuited Turn in a PMSM Through Current Harmonic Monitoring," *IEEE Trans. Ind. Electron.*, vol. 58, no. 6, pp. 2565–2568, June 2011, doi: 10.1109/TIE.2010.2060463.

[13] J.A. Rosero, L. Romeral, J. Cusido, A. Garcia and J.A. Ortega, "On the short-circuiting Fault Detection in a PMSM by means of Stator Current Transformations," in *Proc. 2007 IEEE Power Electronics Specialists Conference*, 2007, pp. 1936–1941, doi: 10.1109/PESC.2007.4342300.

[14] P. Pietrzak and M. Wolkiewicz, "Comparison of Selected Methods of the Stator Winding Condition Monitoring of a PMSM Using the Stator Phase Current". *Energies* 2021, vol. 14, no. 6, p. 1630.

[15] M. Zafarani, E. Bostanci, Y. Qi, T. Goktas and B. Akin, "Interturn Short-Circuit Faults in Permanent Magnet Synchronous Machines: An Extended Review and Comprehensive Analysis, *IEEE J. Emerging Sel. Top. Power Electron.*, vol. 6, no. 4, pp. 2173–2191, Dec. 2018, doi: 10.1109/JESTPE.2018.2811538.

[16] A. Maqsood, D. Oslebo, K. Corzine, L. Parsa and Y. Ma, "STFT Cluster Analysis for DC Pulsed Load Monitoring and Fault Detection on Naval Shipboard Power Systems," *IEEE Trans. Transp. Electrif.*, vol. 6, no. 2, pp. 821–831, June 2020, doi: 10.1109/TTE.2020.2981880.

[17] C.H. Park, J. Lee, G. Ahn, M. Youn and B.D. Youn, "Fault Detection of PMSM under Non-Stationary Conditions Based on Wavelet Transformation Combined with Distance Approach," in *Proc. 2019 IEEE 12th International Symposium on Diagnostics for Electrical Machines, Power Electronics and Drives (SDEMPED)*, Toulouse, France, 2019, pp. 88–93, doi: 10.1109/DEMPED.2019.8864842.

[18] J. Hang, J. Zhang, M. Xia, S. Ding and W. Hua, "Inter-turn Fault Diagnosis for Model-Predictive-Controlled-PMSM Based on Cost Function and Wavelet Transform," *IEEE Trans. Power Electron.*, vol. 35, no. 6, pp. 6405–6418, June 2020, doi: 10.1109/TPEL.2019.2953269.

[19] J. Rosero, A. Garcia, J. Cusido, L. Romeral and J.A. Ortega, "Fault detection by means of Hilbert Huang Transform of the stator current in a PMSM with demagnetization," in *Proc. 2007 IEEE International Symposium on Intelligent Signal Process.*, 2007, pp. 1–6, doi: 10.1109/ WISP.2007.4447631.

[20] J. Rosero, L. Romeral, J.A. Ortega and E. Rosero, "Short circuit fault detection in PMSM by means of empirical mode decomposition(EMD) and wigner ville distribution (WVD)," in *Proc. 2008 Twenty-Third Annual IEEE Applied Power Electronics Conference and Exposition*, 2008, pp. 98–103, doi: 10.1109/ APEC.2008.4522706.

[21] Z. Dogan and K. Tetik, "Diagnosis of Inter-Turn Faults Based on Fault Harmonic Component Tracking in LSPMSMs Working Under Nonstationary Conditions," in *IEEE Access*, vol. 9, pp. 92101–92112, 2021, doi: 10.1109/ACCESS.2021.3092605.

[22] J. Rosero, J. Ortega, J. Urresty, J. Cardenas and L. Romeral, "Stator Short Circuits Detection in PMSM by means of Higher Order Spectral Analysis (HOSA)," *2009 Twenty-Fourth Annual IEEE Applied Power Electronics Conference and Exposition*, 2009, pp. 964–969, doi: 10.1109/APEC.2009.4802779.

[23] S. H. Kia, H. Henao and G. Capolino, "A High-Resolution Frequency Estimation Method for Three-Phase Induction Machine Fault Detection," in *IEEE Trans. Ind. Electron.*, vol. 54, no. 4, pp. 2305–2314, Aug. 2007, doi: 10.1109/TIE.2007.899826.

[24] I. Zamudio-Ramírez *et al.*, "Automatic Diagnosis of Electromechanical Faults in Induction Motors Based on the Transient Analysis of the Stray Flux via MUSIC Methods," in *IEEE Trans. Ind. Appl.*, vol. 56, no. 4, pp. 3604–3613, July-Aug. 2020, doi: 10.1109/TIA.2020.2988002.

[25] P. Ewert, "The Application of the Bispectrum Analysis to Detect the Rotor Unbalance of the Induction Motor Supplied by the Mains and Frequency Converter," *Energies*, vol. 13, no. 11, p. 3009, Jun. 2020.

[26] L. Saidi, F. Fnaiech, G. Capolino and H. Henao, "Stator current bi-spectrum patterns for induction machines multiple-faults detection," *IECON 2012 – 38th Annual Conference on IEEE Industrial Electronics Society*, 2012, pp. 5132–5137, doi: 10.1109/IECON.2012.6388975.

[27] F. Gu, Y. Shao, N. Hu, A. Naid and A.D. Ball, "Electrical motor current signal analysis using a modified bispectrum for fault diagnosis of downstream mechanical equipment," *Mech. Syst. Sig. Process.*, vol. 25, no. 1, pp. 360–372, 2011.

[28] P. Ewert and M. Jaworski, "Application of selected higher-order methods to detect rotor unbalance of drive system with PMSM," *2021 IEEE 19th International Power Electronics and Motion Control Conference (PEMC)*, 2021, pp. 874–879, doi: 10.1109/PEMC48073. 2021.9432610.

10

Bull. Pol. Acad. Sci. Tech. Sci., vol. 70, no. 2, p. e140556, 2022

[29] S. Shao, R. Yan, Y. Lu, P. Wang and R.X. Gao, "DCNN-Based Multi-Signal Induction Motor Fault Diagnosis," *IEEE Trans. Instrum. Meas.*, vol. 69, no. 6, pp. 2658–2669, June 2020, doi: 10.1109/TIM. 2019.2925247.

[30] M. Sohaib and J. Kim, "Fault Diagnosis of Rotary Machine Bearings Under Inconsistent Working Conditions," in *IEEE Trans. Instrum. Meas.*, vol. 69, no. 6, pp. 3334–3347, June 2020, doi: 10.1109/TIM.2019.2933342.

[31] X. Pang, X. Xue, W. Jiang and K. Lu, "An Investigation Into Fault Diagnosis of Planetary Gearboxes Using A Bispectrum Convolutional Neural Network, " in *IEEE/ASME Trans. Mechatron.*, vol. 26, no. 4, pp. 2027–2037, 2021, doi: 10.1109/TMECH.2020.3029058.

[32] D.K. Soother *et al.*, "The Importance of Feature Processing in Deep-Learning-Based Condition Monitoring of Motors," *Math. Probl. Eng.*, vol. 2021, p. 9927151, May 2021, doi: 10.1155/2021/9927151.

[33] N. Arthur and J. Penman, "Induction machine condition monitoring with higher order spectra," in *IEEE Trans. Ind. Electron.*, vol. 47, no. 5, pp. 1031–1041, Oct. 2000, doi: 10.1109/41.873211.

[34] K. Hasselmann, W. Munk and G. Macdonald, "Bispectra of ocean waves," in *Proceedings of Symposium on Time Series Analysis*, pp. 125–139, June 1962.

[35] C.R.P. Courtney, S.A. Neild, P.D. Wilcox, B.W. Drinkwater, "Application of the bispectrum for detection of small nonlinearities excited sinusoidally," in *J. Sound Vib.*, vol. 329, no. 10, pp. 4279–4293, Oct. 2010.

[36] M.E. Iglesias-Martínez, P. Fernández de Córdoba, J.A. Antonino-Daviu and J. Alberto Conejero, "Bispectrum Analysis of Stray Flux Signals for the Robust Detection of Winding Asymmetries in Wound Rotor Induction Motors," *2020 IEEE Energy Conversion Congress and Exposition (ECCE)*, 2020, pp. 4485–4490, doi: 10.1109/ECCE44975.2020.9235360.

[37] M. Iglesias-Martínez, J. Antonino-Daviu, P. Fernández de Córdoba, and J. Conejero, "Rotor Fault Detection in Induction Motors Based on Time-Frequency Analysis Using the Bispectrum and the Autocovariance of Stray Flux Signals," in *Energies*, vol. 12, no. 4, p. 597, Feb. 2019.

[38] I.I. Jouny and R.L. Moses, "The bispectrum of complex signals: definitions and properties," in *IEEE Trans. Signal Process.*, vol. 40, no. 11, pp. 2833–2836, Nov. 1992, doi: 10.1109/78.165675.

[39] A. Paz Parra, M.C. Amaya Enciso, J. Olaya Ochoa and J.A. Palacios Peñaranda, "Stator fault diagnosis on squirrel cage induction motors by ESA and EPVA," in *Proc. 2013 Workshop on Power Electronics and Power Quality Applications (PEPQA)*, 2013, pp. 1–6, doi: 10.1109/PEPQA.2013.6614937.